ChemComm

Peroxosolvate Discovery Method Leads to First Cocrystal with Three Energetic Components

Journal:	*ChemComm*
Manuscript ID	CC-COM-04-2022-002024.R1
Article Type:	Communication

COMMUNICATION

Peroxosolvate Discovery Method Leads to First Cocrystal with Three Energetic Components

Michael K. Bellas[a] and Adam J. Matzger*[a]

Received 00th January 20xx,
Accepted 00th January 20xx

DOI: 10.1039/x0xx00000x

In spite of their exceptional performance, energetic peroxosolvates are rare. Research in this area is slowed by the poor availibility of concentrated hydrogen peroxide solutions. Presented here is an efficient peroxosolvate discovery method that is applied in the discovery of the first ternary cocrystal comprising only energetic components.

Hydrogen peroxide (H_2O_2) adducts, peroxosolvates, find application in industry,[1] the medical/dental fields,[1] pharmaceuticals,[2] synthesis,[3] and energetic materials (EM).[4–8] As such, the intermolecular solid-state interactions of H_2O_2 are actively researched and models for peroxosolvate discovery are emerging.[9–12] Among these, the analysis of hydrogen bonding (H-bond) interactions within reported hydrate structures to identify targets for peroxosolvate formation has shown some success.[13] EM research is particularly well-poised to take advantage of this model. Many otherwise promising EMs have been hamstrung by their propensity for hydrate formation, which is viewed as negative due to its detrimental effects on density and performance.[14] Peroxosolvate formation, in these instances, would alleviate the negative effects arising from H_2O incorporation. Additionally, introducing a positive oxygen balance (*OB*) material, like H_2O_2 (+47%), into the crystal lattice of an EM can improve materials properties and energetic performance.[4,15] A negative (-) *OB* indicates that there is insufficient oxygen to completely oxidize the EM (most EMs have -*OB*, Figure 1a) and a positive (+) *OB* indicates an excess of oxygen; *OB* is closely correlated to detonation velocity (D_v) and detonation pressure (P), which are the two most common metrics by which an EM is quantitatively evaluated.[16] These benefits of peroxosolvate formation are supported by calculations suggesting that a CL-20 peroxosolvate was the most powerful non-nuclear explosive ever synthesized,[4] a claim that has since been supported by experimental measurement.[6] One potential hurdle in the application of the hydrogen bond analysis model is the occurrence of isostructural hydrate/peroxosolvate materials. A recent work cataloguing reported peroxosolvate crystal structures noted that in many isostructural systems the peroxosolvate does not form unless highly concentrated, or anhydrous, H_2O_2 solutions are used.[10] Currently, very few isostructural peroxosolvates exist and it has been suggested that such systems are susceptible to isomorphous substitution of H_2O which can impact stability and purity.[10] However, the first examples of isostructural energetic peroxosolvates (two forms of CL-20:H_2O_2)[4] are stable and attainable in high purity. The low number of reported isostructural peroxosolvates may be because they can be missed experimentally if highly concentrated H_2O_2 is not accessible; this is often the case and the preparation/handling of highly concentrated H_2O_2 can be hazardous.[17,18] A way to sidestep this challenge is generating anhydrous H_2O_2 solutions using inexpensive (<$0.10/g) urea:$H_2O_2$ as the H_2O_2 source. While anhydrous H_2O_2 solutions for peroxosolvate formation have been prepared using serine:H_2O_2,[19] this reagent is not commercially available and was prepared from ≥70 wt.% (aq) H_2O_2 solutions.[17] There have been no prior reports of using urea:H_2O_2 in the successful synthesis of organic peroxosolvates.[20,21] Ideally, this approach would limit the synthesis and/or use of highly concentrated H_2O_2 to situations in which peroxosolvate formation has already been verified and phase-pure samples are required. Here, the viability of this approach is demonstrated and two novel energetic peroxosolvates, including the first ternary cocrystal comprising only energetic components, are reported.

In order to evaluate the efficacy of the urea:H_2O_2 method, two proof of concept systems were selected from a recent report: 2-methyl quinoline N-oxide (MQNO) and 4-(3-phenyl propyl)pyridine N-oxide (3PNO) (Figure 1a).[13] For both MQNO and 3PNO, the peroxosolvates were obtained via evaporative crystallization from urea:H_2O_2 acetonitrile solution (urea:H_2O_2 acetonitrile solution is referred to as UHPA here), albeit with residual urea:H_2O_2, as verified by Raman microscopy (Figure 1b). Transitioning to applying the UHPA method in novel peroxosolvate discovery efforts required several guiding criteria for coformer selection. Peroxosolvate formation is driven by H-bonding interactions. While traditional (C,H,N,O) EMs commonly lack strong hydrogen bonding functionality, high-

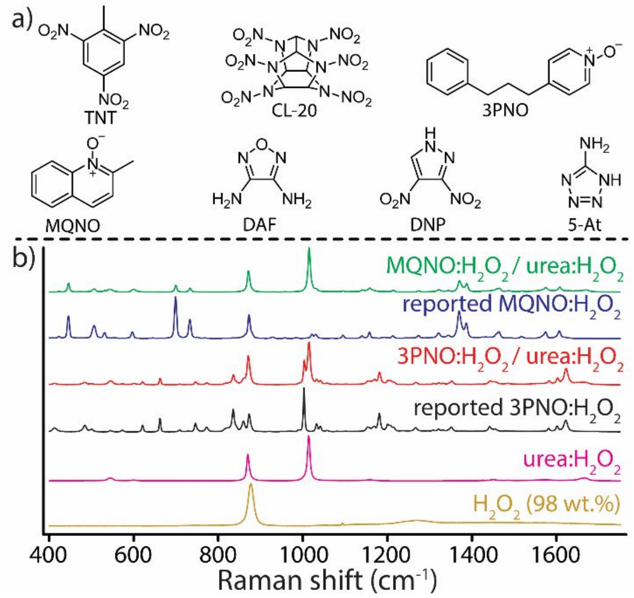

Figure 1 a) structures of relevant EMs, 3PNO, and MQNO. b) Raman spectra for the 3PNO and MQNO peroxosolvates, urea:H_2O_2, and 98 wt% H_2O_2.

nitrogen EMs often contain good H-bond accepting functionality making these materials well-suited for interacting with H_2O_2. Thus, simple commercially available high nitrogen molecules were targeted. Additionally, there are now numerous reports of peroxosolvate forming molecules having been identified through inspection of their known hydrate structures.[9] However, the mere existence of a hydrate is no guarantee that a peroxosolvate can be obtained. It is now known that the odds of successful peroxosolvate formation are greater when the corresponding hydrate has H_2O H-bond donation exceeding H-bond accepting interactions.[10] In such situations the greater H-bond donating ability of H_2O_2 can be leveraged to achieve peroxosolvates. The contrast and comparison of H-bonding interactions of H_2O and H_2O_2 has been discussed extensively elsewhere and the greater H-bond donating ability of H_2O_2 is supported by calculations[22,23] and reflected in its greater acidity.[1] Having limited our scope to simple, commercially available, high-nitrogen materials, with known hydrates in which H_2O acts primarily as a H-bond donor, 5-aminotetrazole (5-At, Figure 1a) was identified as an ideal candidate material.

Applying the UHPA method to 5-At results in a physical mixture including crystals of a material demonstrating a signal in a region of the Raman spectrum where an H_2O_2 O-O stretch is expected (Figure 2a). Encouraged by this result, 5-At was dissolved in 50 wt.% H_2O_2(aq) and the solution subsequently evaporated. This experiment, however, only afforded 5-At and 5-At-monohydrate (5-AtH). The experimental results thus far suggested the possibility that an isostructural peroxosolvate may exist, warranting experimentation with more concentrated 98% H_2O_2. As suspected, the use of concentrated H_2O_2 provided phase-pure 5-At-peroxosolvate (5-AtP). Formation of the 5-AtP was verified using Raman microscopy (Figure 2a), powder X-ray diffraction (PXRD) (see SI), and single crystal X-ray diffraction (SCXRD), which also showed a high degree of structural similarity between the hydrate and peroxosolvate (Figure 2b). There are, however, notable differences between H_2O_2 and H_2O positions in the structures and H_2O_2 molecules are disordered over two positions.

Encouraged by the success of this approach in the 5-At system, a more challenging system was targeted. Ternary cocrystals, and their rational design, represent a promising emerging class of compounds in contemporary crystal engineering literature.[24,25] Recently, an energetic-energetic cocrystal hydrate (DDH) composed of 3,4-diaminofurazan (DAF) and 3,4-dinitropyrazole (DNP) (Figure 1a) was reported by Zhang et. al.[26] that nicely illustrates the potential to move EMs beyond two components. In that report, the researchers recognized the potential for peroxosolvate formation and made numerous attempts to synthesize the peroxosolvate, all of which failed. This outcome surprised us and the potential to produce the first cocrystal containing three energetic components was too enticing not to revisit this material. In DDH, H_2O donates two H-bonds to traditionally strong H-bond acceptors while one of the H-bond accepting interactions is via a non-classical C-H donor (Figure 3a), i.e., H_2O has better H-bond donating than accepting interactions. Additionally, the spatial arrangement of the H-bond donating/accepting functionalities in DDH are such that exchanging the H-bonding interactions with H_2O for interactions with H_2O_2 may be possible without disrupting broader packing arrangement. Though lattice expansion and/or rearrangement precludes a specific requirement for the volume

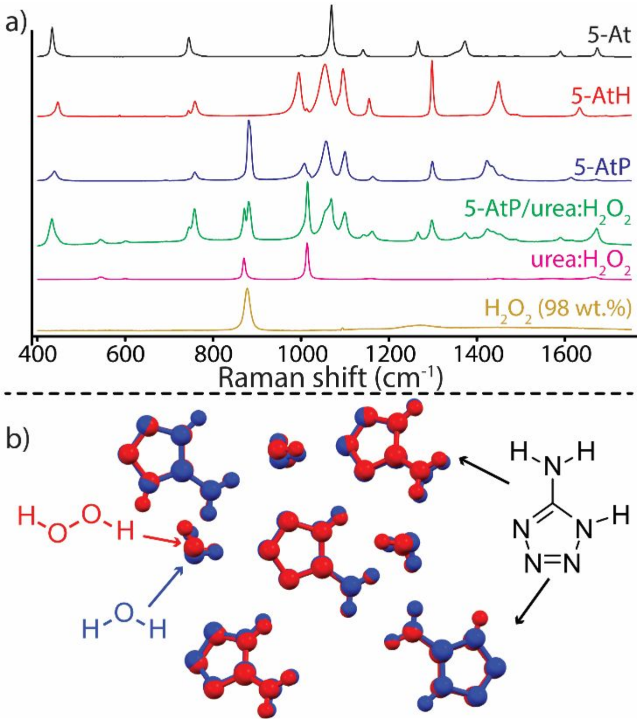

Figure 2 a) Raman spectra for the 5-At system. b) structural overlay of 5-AtP (red) and 5-AtH (blue), H_2O_2 is di

---

[a] Department of Chemistry, University of Michigan
930 N. University Ave., Ann Arbor, MI 48109-1055 (USA)

Electronic Supplementary Information (ESI) available: details concerning synthesis, characterization, calculations, and data curation/analysis. See DOI: 10.1039/x0xx00000x

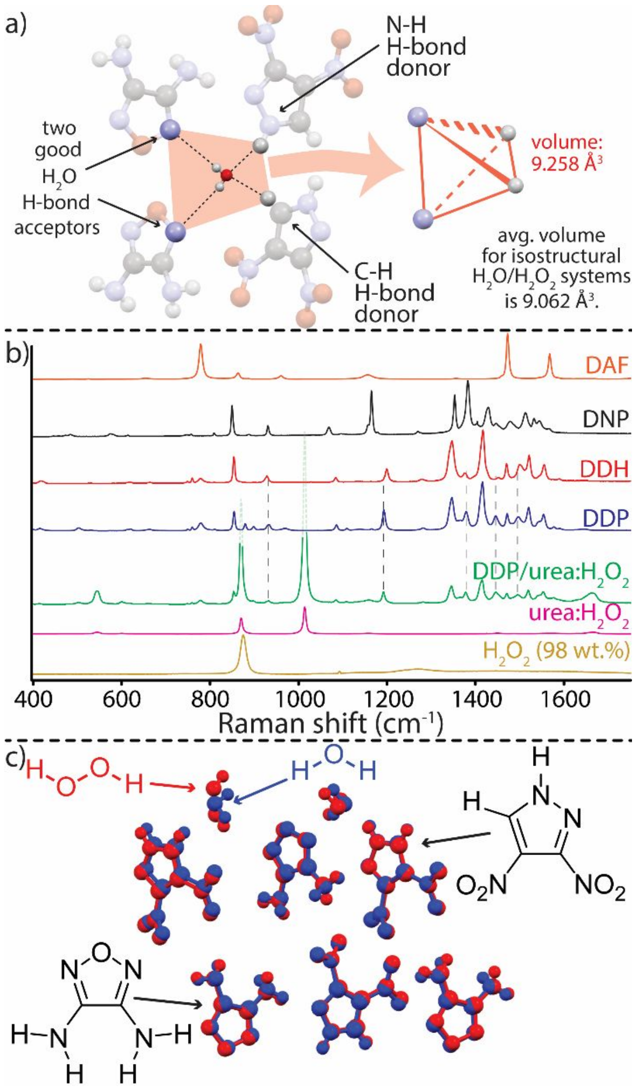

Figure 3 a) Diagram of the H_2O H-bonding environment in DDH and an illustration of the available volume for H_2O/H_2O_2 molecules. b) Raman spectra for the DAF-DNP system, guidelines added to aid the reader. c) structural overlay of DDP (red) and DDH (blue).

available to H_2O_2 when applying the hydrate analysis method in pursuit of peroxosolvates, it was noted that the volume encompassing the H-bonding interactions with H_2O was within the range seen in other hydrated structures which have an isostructural peroxosolvate (Figure 3a).[10] This analysis suggested that perhaps the peroxosolvate, if achievable, would be isostructural and may require dry conditions for formation. Thus, the UHPA method was applied to the DDH system. By this method the first ternary cocrystal comprised entirely of energetic components was discovered. This material (DDP) is composed of DAF, DNP, and H_2O_2 in a 1:1:1 stoichiometry. Initial discovery was made by Raman microscopy (Figure 3b) and a phase pure sample, as determined using PXRD (see SI), was then obtained using 98% H_2O_2. As can be seen in the molecular overlay, the hydrate and peroxosolvate are indeed isostructural (Figure 3c). Using Mercury software,[27] structural similarity calculations were carried out and the hydrate/peroxosolvate structures show a 96% similarity. To corroborate the need for exclusion of water in isostructural peroxosolvate formation experiments, DDP formation was attempted using 50 wt.% H_2O_2(aq) and no DDP was detected.

The thermal properties of an EM are critical in determining possible applications. Developing a general understanding of how the thermal properties of an EM might change upon isostructural H_2O_2/ H_2O exchange assists identification of target systems for peroxosolvate formation. The thermal properties of the novel peroxosolvates reported here, as well as their constituent materials and reported hydrates, were characterized via thermogravimetric analysis (TGA) and differential scanning calorimetry (DSC). The TGA data for the 5-At system (Figure 4a) shows that dehydration/desolvation occurs at relatively low temperature. Following this event, the components of the 5-At system all show decomposition beginning in the range 202-204 °C. DSC data (Figure 4b) shows that 5-AtP melts with decomposition beginning at 90.1 °C.

The TGA thermograms for the DAF-DNP system (Figure 4c) show a similar trend to that in the 5-At system. Following dehydration, DDH undergoes further decomposition beginning at 121 °C while the post-desolvation decomposition of DDP begins at 132 °C. By DSC, DDH shows an endotherm beginning at 71.6 °C (Figure 4d) with the corresponding endotherm for DDP beginning at 86.6 °C. This improvement in thermal stability is also reflected in the exothermic decomposition of DDP which begins at 168.3 °C (by DSC), >14 °C higher than observed for DDH (153.8 °C).

The energetic performance criteria for these systems were calculated using Cheetah 7.0, a thermochemical code used for calculating the performance of energetic materials. Along with *OB*, density is an important indicator of energetic performance. Furthermore, analysis of a compilation[10] of peroxosolvates and their isostructural hydrates revealed that peroxosolvate formation is an effective method to improve upon the density of materials, with an average increase in density of ca. 4% (see

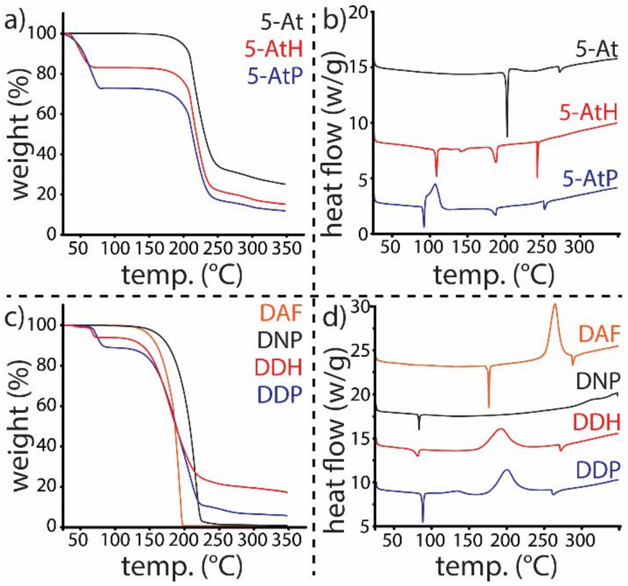

Figure 4 TGA thermograms for the 5-At system a) and DAF-DNP system c) as well as DSC thermograms for the 5-At system b) and DAF-DNP system d).

Table 1 Room temperature crystallographic densities, detonation velocities, detonation pressures, and oxygen balance for relevant materials. *5-AtP melts with decomposition. **The thermal decomposition of 5-AtH is not defined by a single temperature.

	5-AtH	**5-AtP**	**DDH**	**DDP**
***d* (*g*/*cm*^{3})**	1.486	1.538	1.683	1.715
D_v (*km*/*s*)	7.04	7.90	7.77	8.04
P_{cj} (*GPa*)	15.8	21.5	24.6	27.5
***OB* (*%*)**	-54	-34	-46	-38
$T_{decomp.}$ (°C)	**	90.1*	153.8	168.3

SI). For both systems, peroxosolvate formation improved density, *OB*, and energetic performance relative to the hydrates (Table 1). Safety is indeed always a concern with EMs and the d_{h50} (the height at which a known mass may dropped on the material with a 50% likelihood of detonation) was determined using our in-house apparatus.[28] The d_{h50} for 5-AtP is 14 cm while that of DDP is 38 cm; for reference, the d_{h50} of the well-established EMs 1,3,5,7-tetranitro-1,3,5,7-tetrazocane (β-HMX) and CL-20 (ε-polymorph) are 29 cm and 55 cm respectively on this apparatus. The poor calculated performance criteria, low thermal stability, and dangerously high impact sensitivity overshadow the positive attributes of 5-AtP, from an applications perspective. However, DDP shows a notable improvement, relative to DDH, in many areas and warrants further investigation.

Peroxosolvate formation is a novel technique for improving OB, density, and energetic performance. Though H_2O_2 solutions are not difficult to obtain at low concentrations, highly conc. H_2O_2 solution remains inaccessible to many researchers. As interest in isostructural H_2O_2/ H_2O systems grows, so too will the need for highly conc. or anhydrous H_2O_2 solutions in discovery efforts. The UHPA method provides a safer, inexpensive, and easily accessible alternative to conc. H_2O_2. The viability of this method is demonstrated here and affords novel peroxosolvates not attainable using widely available dilute (or even 50 wt.%) H_2O_2 solutions. This method is also applicable to fields outside of EM research, such as pharmaceuticals,[2] where convenient peroxosolvate discovery methods are sorely needed.

The authors acknowledge the support of the Army Research Office (ARO) (grant number: W911NF-19-1-0114)

Conflicts of interest

The authors declare no conflicting interests.

Notes and references

1 1. H. Jakob, S. Leininger, T. Lehmann, S. Jacobi, S. Gutewort, in *Ullmann's Encyclopedia of Industrial Chemistry*, ed. B. Elvers, Wiley-VCH, Germany, 2007, vol. 26, 293–324.

2 K. M. Kersten, M. E. Breen, A. K. Mapp, A. J. Matzger, *Chem. Commun.* 2018, **54**, 9286–9289.

3 W. Adam, C. M. Mitchell, *Angew. Chem. Int. Ed. Engl.* 1996, **35**, 533–535.

4 J. C. Bennion, N. Chowdhury, J. W. Kampf, A. J. Matzger, *Angew. Chem. Int. Ed. Engl.* 2016, **128**, 13312–13315.

5 J. Luo, H. Xia, W. Zhang, S. Song, Q. Zhang, *J. Mater. Chem. A* 2020, **8**, 12334–12338.

6 V. S. Vuppuluri, J. C. Bennion, R. A. Wiscons, I. E. Gunduz, A. J. Matzger, S. F. Son, *Propellants, Explos., Pyrotech.* 2019, **44**, 313–318.

7 A. V. Churakov, D. A. Grishanov, A. G. Medvedev, A. A. Mikhaylov, M. V. Vener, M. A. Navasardyan, T. A. Tripol'skaya, O. Lev, P. V. Prikhodchenko, *Cryst. Eng. Comm.* 2020, **22**, 2866-2872.

8 Y. Wang, S. Song, C. Huang, X. Qi, K. Wang, Y. Liu, Q. Zhang, *J. Mater. Chem. A* 2019, **7**, 19248-19257.

9 A. G. Medvedev, A. V. Churakov, P. V. Prikhodchenko, O. Lev, M. V. Vener, *Molecules* 2020, **26**, 26.

10 I. Yu. Chernyshov, M. V. Vener, P. V. Prikhodchenko, A. G. Medvedev, O. Lev, A. V. Churakov, *Cryst. Growth Des.* 2017, **17**, 214–220.

11 D. A. Grishanov, M. A. Navasardyan, A. G. Medvedev, O. Lev, P. V. Prikhodchenko, A. V. Churakov, *Angew. Chem. Int. Ed.* 2017, **56**, 15241–15245.

12 R. A. Wiscons, R. Nikhar, K. Szalewicz, A. J. Matzger, *Phys. Chem. Chem. Phys.,* 2022, **24**, 11206-11212.

13 L. M. Foroughi, A. J. Matzger, *Cryst. Growth Des.* 2021, 21, 5873–5879.

14 R. A. Wiscons, M. K. Bellas, J. C. Bennion, A. J. Matzger, *Cryst. Growth Des.* 2018, **18**, 7701–7707.

15 M. K. Bellas, A. J. Matzger, *Angew. Chem. Int. Ed*. 2019, **58**, 17185–17188.

16 T. M. Klapötke, *Chemistry of High-Energy Materials*, De Gruyter, Berlin/Boston, 2012.

17 Y. Wolanov, O. Lev, A. V. Churakov, A. G. Medvedev, V. M. Novotortsev, P. V. Prikhodchenko, *Tetrahedron* 2010, **66**, 5130–5133.

18 Hydrogen Peroxide Accidents and Incidents: What We Can Learn from History, http://mae-nas.eng.usu.edu/Peroxide_Web_Page/documents/lessons_learned_nasa.pdf, (accessed January 2022).

19 A. G. Medvedev, A. A. Mikhaylov, A. V. Churakov, P. V. Prikhodchenko, O. Lev, *Acta Crystallogr., Sect. C: Cryst. Struct. Commun.* 2012, **68**, i20–i24.

20 C. R. Groom, I. J. Bruno, M. P. Lightfoot, S. C. Ward, *Acta Crystallogr., Sect. B: Struct. Sci., Cryst. Eng. Mater.* 2016, **72**, 171–179.

21 This assertion is based on a literature search as well as evaluating the synthetic schemes for the 125 structurally characterized organic peroxosolvates deposited within the Cambridge Structural Database, see SI for details.

22 M. V. Vener, A. V. Churakov, A. P. Voronin, O. D. Parashchuk, S. V. Artobolevskii, O. A. Alatortsev, D. E. Makhrov, A. G. Medvedev, A. Filarowski, *Molecules* 2022, **27**, 717.

23 M. V. Vener, A. G. Medvedev, A. V. Churakov, P. V. Prikhodchenko, T. A. Tripol'skaya, O. Lev, *J. Phys. Chem. A* 2011, **115**, 13657–13663.

24 H. Jain, D. Sutradhar, S. Roy, G. R. Desiraju, *Angew. Chem. Int. Ed.* 2021, **60**, 12841–12846.

25 F. Topić, K. Rissanen, *J. Am. Chem. Soc.* 2016, **138**, 6610–6616.

26 X. Zhang, Y. Wu, S. Jin, G. Lan, X. Wang, J. Wang, F. Shang, S. Chen, J. Du, Q. Shu, *J. Energ. Mater.* 2022, 1–13.

27 C. F. Macrae, I. Sovago, S. J. Cottrell, P. T. A. Galek, P. McCabe, E. Pidcock, M. Platings, G. P. Shields, J. S. Stevens, M. Towler, P. A. Wood, *J Appl Crystallogr* 2020, **53**, 226–235.

28 O. Bolton, L. R. Simke, P. F. Pagoria, A. J. Matzger, *Cryst. Growth Des.* 2012, **12**, 4311–4314.